Integral Formulation for Analysis of Integrated Dielectric Waveguides

JONATHAN S. BAGBY, MEMBER, IEEE, DENNIS P. NYQUIST, MEMBER, IEEE, AND BYRON C. DRACHMAN

Abstract —A polarization integral equation is advanced for use in the conceptual and numerical analysis of a broad class of integrated dielectric waveguiding systems. The equation is applied to axially uniform waveguides, in which case the axial integral becomes convolutional in nature, prompting a Fourier transform on that variable. Inversion of the transformed guiding region field, aided by complex analysis, allows identification of two components of that field: the surface-wave modes and the radiation field. These are found in terms of the sources exciting the system, leading to a new formulation for the excitation of such waveguides. Analysis of the behavior of the kernel of the transformed integral equation in the complex plane leads to a general criterion for surface-wave leakage from the guiding region. Numerical results for the propagation characteristics of step- and the graded-index rectangular strip and rib waveguides are obtained from the integral equation by application of the method of moments and by a quasi-closed-form solution technique. These results are compared to those of other formulations. Further application of the integral equation is discussed, and several promising areas for further study are identified.

I. Introduction

THE PRACTICAL APPLICATION of dielectric waveguides in millimeter-wave integrated circuits depends critically on the propagation characteristics of these waveguides. For this reason, there has been enduring interest in methods of determining these characteristics for practical dielectric waveguiding structures. Exact solutions for the fields in dielectric waveguides exist for few structures, such as the asymmetric slab waveguide [1] and uniformly clad dielectric fibers of circular and elliptic cross section [2]. The boundary conditions at the core/surround interface for other structures are inseparable, rendering differential formulations of the problem insolvable.

Differential formulations have provided the basis for approximate solutions, notably for surface waves along rectangular step-index waveguides. The technique used in the classic study by Marcatili [3] yields good results with minimal effort for large step-index rectangular guides. A potentially exact solution for this structure has been obtained by Goell [4]; however, time and storage considerations yield approximate numerical results. A similar difficulty holds for the potentially exact mode-matching technique of Peng and Oliner *et al.* [5], [6]. The radiation field of the guide is addressed in that work, but the spectrum of radiation eigenvalues is quantized by the introduction of distant conducting boundaries, leading to approximate results. Shortcomings common to the above-mentioned analyses are their inability to incorporate core grading and inapplicability to structures of more general shape. These considerations are of practical importance since waveguiding characteristics may improve with transverse core grading, and fabrication technology renders the construction of rectangular step-index waveguides difficult at best.

In this paper, we utilize a polarization integral equation (EFIE) to analyze a broad class of integrated dieletric waveguides. This integral equation is related to that derived by Katsenelenbaum [7] and used by Livesay and Chen [8]. It was developed by Johnson and Nyquist in [9] and provides a conceptually exact formulation of the electric field in a broad class of integrated waveguiding systems. The integral formulation provides several advantages over conventional differential formulations. Boundary conditions are incorporated in a general manner into the dyadic Green's function kernel; thus, physical phenomena such as mode leakage which may be obscured in conventional formulations (see [5] and [6]) can be treated. The formulation is also valid for arbitrarily-graded waveguides of arbitrary shape.

The remainder of this paper is organized into four sections. In Section II, we briefly sketch the development of the polarization integral equation and present the dyadic Green's function which forms the kernel of the equation. We then specialize the integral equation to axially uniform waveguides by Fourier transforming on the axial variable. In Section III, we develop an excitation theory for axially uniform integrated dielectric waveguides. This theory is based on formal Fourier inversion of the unknown transformed waveguide field. Analysis of the EFIE in the complex transform variable plane allows characterization of the complete modal spectral of this class of waveguides: Surface waves are associated with a residue series at poles enclosed by the inversion contour, and the radiation field is associated with branch integrals required by the presence of

Manuscript received February 3, 1985; revised June 3, 1985. This work was supported in part by the National Science Foundation under Grant ECS-8311038.

J. S. Bagby is with the Department of Electrical Engineering, University of Texas at Arlington, Arlington, TX 70619.

D. P. Nyquist is with the Department of Electrical Engineering and Systems Science, Michigan State University, East Lansing, MI 48824.

B. C. Drachman is with the Department of Mathematics, Michigan State University, East Lansing, MI 48824.

0018-9480/85/1000-0906$01.00 ©1985 IEEE

multivalued parameters in the integrand. The surface waves are shown to satisfy the homogeneous form of the transformed EFIE, and the radiation field is shown to consist of a two-dimensional superposition of spectral components which satisfy a forced EFIE. This analysis provides the excitation amplitudes of the surface-wave modes and the radiation field spectral components in terms of the incident excitatory field. Another important result is the ability of this analysis to describe the physical phenomenon of guided mode leakage [5], [6]. In Section IV, we apply the integral equation to the determination of propagation characteristics of step- and graded-index rectangular waveguides. Two techniques are used: we implement a moment method solution to the integral equation, and we also use a quasi-closed-form solution technique. Numerical results are presented and compared to those of other formulations. We close, in Section V, with a discussion of our applications of the polarization integral equation, and several promising areas for further study are identified.

II. Mathematical Formulation

In this section, we present a polarization electric-field integral equation for a generalized integrated dielectric waveguiding system. This integral equation provides the mathematical formulation for the remainder of this paper.

The physical system that the EFIE is applicable to is depicted in Fig. 1. It consists of an inhomogeneous dielectric waveguide core located in the top layer of a three-layer uniform dielectric background region intended to represent the substrate, film, and cover regions of typical integrated dielectric waveguides. Excitation is provided by an impressed electric field $\vec{E}^i$ maintained by current $\vec{J}^e = j\omega\vec{P}^e$ associated with a primary polarization source $\vec{P}^e$ immersed in the cover region of the layered background. That impressed field is scattered by the inhomogeneous guiding region, due to the contrast $\delta n^2(\vec{r}) = n^2(\vec{r}) - n_c^2$ of its refractive index against that of the uniform cover, resulting in a scattered field $\vec{E}^s$. The total field at any point in the system is $\vec{E} = \vec{E}^i + \vec{E}^s$. The scattered field is maintained by the equivalent induced polarization $\vec{P}_{eq} = \delta n^2(\vec{r})\epsilon_0\vec{E}(\vec{r})$. Solution of this scattering problem requires the determination of $\vec{E}$ at all points $\vec{r} \in V$, where V is that region where $\delta n^2 \neq 0$. The polarization sources radiate in the presence of the tri-layered cover/film/substrate background region; treatment of this problem involves the electromagnetics of layered media.

The field maintained by the total effective polarization in the cover region can be expressed through electric Hertzian potentials by a generalization of Sommerfeld's classic method [10]. The result is

$$\vec{E}(\vec{r}) = \left(k_c^2 + \nabla\nabla\cdot\right)\int_V \overleftrightarrow{G}(\vec{r}|\vec{r}')\cdot\frac{\vec{P}^e(\vec{r}') + \vec{P}_{eq}(\vec{r}')}{\epsilon_c}\,dV' \tag{1}$$

where $k_l = n_l k_0$ for $l = c$, f, or s for the cover, film, or substrate regions, respectively, and k_0 is the free-space wavenumber. Here $\vec{E}^i$ is the impressed field maintained by

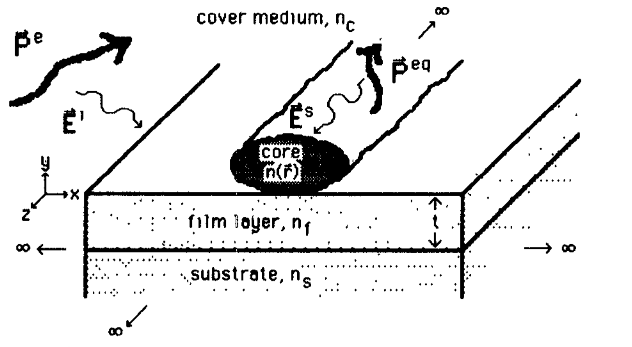

Fig. 1. Generalized integrated dielectric waveguide consisting of an arbitrarily graded waveguiding region adjacent to a film/cover interface over a uniform substrate.

$\vec{P}^e$, $\vec{E}^s$ is the scattered field maintained by $\vec{P}_{eq} = \delta n^2\epsilon_0\vec{E}$, and $\overleftrightarrow{G}$ is a Hertzian potential Green's dyadic. Rearranging (1) leads to an EFIE for the field maintained in the waveguide by the impressed field $\vec{E}^i$ as

$$\vec{E}(\vec{r}) - \left(k_c^2 + \nabla\nabla\cdot\right)\int_V \frac{\delta n^2(\vec{r}')}{n_c^2}\overleftrightarrow{G}(\vec{r}|\vec{r}')\cdot\vec{E}(\vec{r}')\,dV' = \vec{E}^i(\vec{r}), \qquad \vec{r} \in V. \tag{2}$$

An alternative form of EFIE, (2) is useful in analytical developments; it is obtained in terms of an electric Green's dyad $\overleftrightarrow{G}_e$. If the differential operator in (2) is passed through the integral to operate on $\overleftrightarrow{G}$, the singularity of the Hertzian potential Green's dyad is rendered nonintegrable and integration must be performed in the principal value sense. This results in the introduction of a nonphysical source due to exclusion of the principal volume which must be subsequently subtracted by use of a depolarizing dyad $\overleftrightarrow{L}$ [11]. These considerations lead to the definition of the electric Green's dyad

$$\overleftrightarrow{G}_e(\vec{r}|\vec{r}') = P.V.\left(k_c^2 + \nabla\nabla\cdot\right)\overleftrightarrow{G}(\vec{r}|\vec{r}') + \overleftrightarrow{L}\delta(\vec{r} - \vec{r}). \tag{3}$$

An alternative form of the EFIE for $\vec{E}$ excited by $\vec{E}^i$ is thus

$$\vec{E}(\vec{r}) - \int_V \frac{\delta n^2(\vec{r}')}{n_c^2}\overleftrightarrow{G}_e(\vec{r}|\vec{r}')\cdot\vec{E}(\vec{r}')\,dV' = \vec{E}^i(\vec{r}), \qquad \vec{r} \in V. \tag{4}$$

The Hertzian potential Green's dyad decomposes into a principal and reflected part $\overleftrightarrow{G} = \overleftrightarrow{G}^p + \overleftrightarrow{G}^r$, where

$$\overleftrightarrow{G}^p(\vec{r}|\vec{r}') = \overleftrightarrow{I}G^p(\vec{r}|\vec{r}')$$
$$\overleftrightarrow{G}^r(\vec{r}|\vec{r}') = \hat{x}G_t^r\hat{x} + \hat{y}\left\{\frac{\partial}{\partial x}G_c^r\hat{x} + G_n^r\hat{y} + \frac{\partial}{\partial z}G_c^r\hat{z}\right\} + \hat{z}G_t^r\hat{z}. \tag{5}$$

Potential components tangential to background interfaces excited by tangential sources are described through G_t^r and normal potentials due to normal sources are obtained from G_n^r, while the coupling component G_c^r yields the normal potential maintained by tangential sources. The various

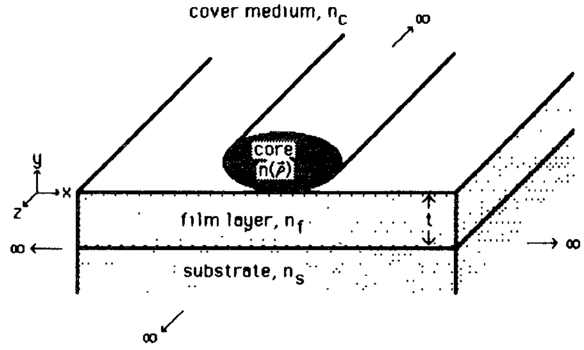

Fig. 2. Axially uniform integrated dielectric waveguide in a tri-layered background environment.

components of the Green's dyad are found in terms of Sommerfeld integrals

$$G^p(\vec{r}|\vec{r}') = \iint_{-\infty}^{\infty} \frac{e^{j\vec{\lambda}\cdot(\vec{r}-\vec{r}')}e^{-p_c|y-y'|}}{2(2\pi)^2 p_c} d^2\lambda = \frac{e^{-jk_c|\vec{r}-\vec{r}'|}}{4\pi|\vec{r}-\vec{r}'|}$$

$$\left.\begin{matrix} G_t^r(\vec{r}|\vec{r}') \\ G_n^r(\vec{r}|\vec{r}') \\ G_c^r(\vec{r}|\vec{r}') \end{matrix}\right\} = \iint_{-\infty}^{\infty} \left\{\begin{matrix} R_t(\lambda) \\ R_n(\lambda) \\ C(\lambda) \end{matrix}\right\} \frac{e^{j\vec{\lambda}\cdot(\vec{r}-\vec{r}')}e^{-p_c(y+y')}}{2(2\pi)^2 p_c} d^2\lambda \quad (6)$$

where $\vec{\lambda} = \xi\hat{x} + \zeta\hat{z}$, $\lambda^2 = \xi^2 + \zeta^2$, $d^2\lambda = d\xi d\zeta$, and $p_l^2 = \lambda^2 - k_l^2$ for $l = c$, f, or s. The reflection coefficients R_t and R_n are associated with tangential and normal potential components, while C is a coupling coefficient; these coefficients depend on the parameters of the cover/film/substrate background in a complicated manner, as indicated in the accompanying Appendix.

In case of an axially uniform guide such as that shown in Fig. 2, the refractive index contrast factor is a function of transverse position only, or $\delta n^2(\vec{r}) = \delta n^2(\vec{\rho})$ with $\vec{\rho} = x\hat{x} + y\hat{y}$. We also note that $\overleftrightarrow{G}(\vec{r}|\vec{r}') = \overleftrightarrow{G}(\vec{\rho}|\vec{\rho}'; z - z')$; in this case, the axial integral in (2) is convolutional in nature, prompting a Fourier transformation on that variable. This leads to an EFIE for the transformed field $\vec{e}$ of an axially uniform waveguide due to a transformed impressed field $\vec{e}^i$

$$\vec{e}(\vec{\rho},\zeta) - (k_c^2 + \tilde{\nabla}\tilde{\nabla}\cdot) \cdot \int_{CS} \frac{\delta n^2(\vec{\rho}')}{n_c^2} \overleftrightarrow{g}_\zeta(\vec{\rho}|\vec{\rho}')\cdot\vec{e}(\vec{\rho}',\zeta)\, dS' = \vec{e}^i(\vec{\rho},\zeta), \quad \vec{\rho} \in CS \quad (7)$$

where ζ is the transform variable and $\tilde{\nabla} = \nabla_t + j\zeta\hat{z}$.

The transformed Green's dyad $\overleftrightarrow{g}_\zeta$ decomposes as previously, with

$$\overleftrightarrow{g}_\zeta(\vec{\rho}|\vec{\rho}') = \overleftrightarrow{g}_\zeta^p(\vec{\rho}|\vec{\rho}') + \overleftrightarrow{g}_\zeta^r(\vec{\rho}|\vec{\rho}'), \qquad \overleftrightarrow{g}_\zeta^p = \overleftrightarrow{I} g_\zeta^p$$

$$\overleftrightarrow{g}_\zeta^r(\vec{\rho}|\vec{\rho}') = \hat{x} g_{\zeta t}^r \hat{x} + \hat{y}\left\{\frac{\partial}{\partial x} g_{\zeta c}^r \hat{x} + g_{\zeta n}^r \hat{y} + j\zeta g_{\zeta t}^r \hat{z}\right\} + \hat{z} g_{\zeta c}^r \hat{z}. \quad (8)$$

Integral representations of the scalar components are given by

$$g_\zeta^p(\vec{\rho}|\vec{\rho}') = \int_{-\infty}^{\infty} \frac{e^{j\xi(x-x')}e^{-p_c|y-y'|}}{4\pi p_c} d\xi = \frac{1}{2\pi} K_0(\gamma_c|\vec{\rho}-\vec{\rho}'|)$$

$$\left.\begin{matrix} g_{\zeta t}^r(\vec{\rho}|\vec{\rho}') \\ g_{\zeta n}^r(\vec{\rho}|\vec{\rho}') \\ g_{\zeta c}^r(\vec{\rho}|\vec{\rho}') \end{matrix}\right\} = \int_{-\infty}^{\infty} \left\{\begin{matrix} R_t(\lambda) \\ R_n(\lambda) \\ C(\lambda) \end{matrix}\right\} \frac{e^{j\xi(x-x')}e^{-p_c(y+y')}}{4\pi p_c} d\xi \quad (9)$$

with $\lambda^2 = \xi^2 + \zeta^2$, $\gamma_l^2 = \zeta^2 - k_l^2$, and $p_l^2 = \lambda^2 - k_l^2$ for $l = c, f, s$.

The integrals in (9) can be transformed to alternative forms by complex plane analysis. For fixed ζ, the p_l introduce branch point singularities in the complex ξ plane. If the real axis integrals are closed along semicircles of infinite radius in the upper or lower half planes, it is necessary to detour along branch cuts emanating from points $\pm j\gamma_l$; these cuts follow the usual hyperbolic paths in the ξ plane (see [12], [13]) to guarantee the vanishing of contributions from the infinite semicircular path. It can be shown [12] that the coefficients R_t, R_n, and C in (9) are singular at such ξ where the p_l correspond to TE and TM surface-wave eigenvalues of the background asymmetric slab waveguide (see discussion in Section III). These considerations lead to useful alternative representations of the Green's function components in terms of a residue series at these poles plus branch integral contributions.

It is convenient in conceptual developments to exploit a modified version of EFIE (7). An alternative transformed EFIE is obtained as

$$\vec{e}(\vec{\rho},\zeta) - \int_{CS} \frac{\delta n^2(\vec{\rho}')}{n_c^2} \overleftrightarrow{g}_{e\zeta}(\vec{\rho}|\vec{\rho}')\cdot\vec{e}(\vec{\rho}',\zeta)\, dS' = \vec{e}^i(\vec{\rho},\zeta), \qquad \vec{\rho} \in CS \quad (10)$$

where the transformed electric Green's dyad is $\overleftrightarrow{g}_{e\zeta}(\vec{\rho}|\vec{\rho}') = P.V.(k_c^2 + \tilde{\nabla}\tilde{\nabla}\cdot)\overleftrightarrow{g}_\zeta(\vec{\rho}|\vec{\rho}') + \overleftrightarrow{l}\delta(\vec{\rho}-\vec{\rho}')$ and $\overleftrightarrow{l}$ is the two-dimensional depolarizing dyad [11].

III. Transform Plane Analysis

In this section, we consider the excitation of axially uniform integrated dielectric waveguides. The analysis is based on formal Fourier inversion of the transformed total field in the waveguide.

The total field in the core of an axially uniform integrated waveguide is given by

$$\vec{E}(\vec{\rho},z) = \frac{1}{2\pi}\int_{-\infty}^{\infty} \vec{e}(\vec{\rho},\zeta)e^{j\zeta z} d\zeta \quad (11)$$

where $\vec{e}(\vec{\rho},\zeta)$ satisfies (10). We will perform this inversion with the aid of complex analysis. Modify the real line integral in (11) to form a closed path in the complex ζ plane. An infinite semicircular contour $\mathscr{C}_\infty$ extends into the upper or lower half plane depending on the sign of $z - z'$, as illustrated in Fig. 3. Since $\vec{e}$ is the solution of (10), it shares the ζ plane branch point singularities of $\overleftrightarrow{g}_{e\zeta}$ arising from the $p_l = (\xi^2 + \zeta^2 - k_l^2)^{1/2}$ for $l = c$ or s (k_f is not implicated since the integrands of $\overleftrightarrow{g}_\zeta^r$ are even in p_f;

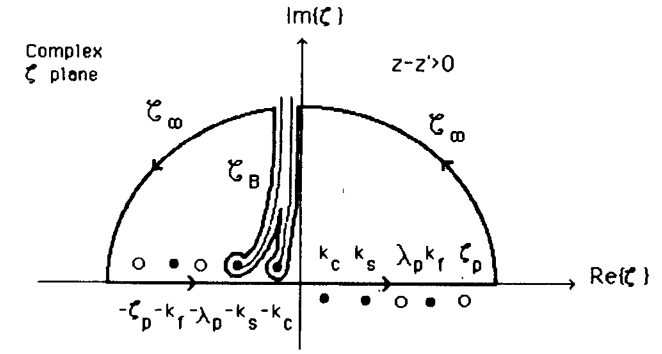

Fig. 3. Singularities of the transformed core field and the deformed inversion contour to aid in identification of the model spectrum of an integrated waveguide.

see the Appendix). We choose hyperbolic branch cuts eminating from the branch points $\zeta = \pm k_l$ to assure convergence along $\mathscr{C}_\infty$. The contour may also enclose pole singularities of $\vec{e}$ at $\zeta = \zeta_p$. We thus have

$$\vec{E}(\vec{\rho}, z) = \frac{1}{2\pi}\left\{2\pi j \sum_p \operatorname*{Res}_{\zeta_p}\left[\vec{e}(\vec{\rho},\zeta)e^{j\zeta z}\right] \cdot \int_{\mathscr{C}_B} \vec{e}(\vec{\rho},\zeta)e^{j\zeta z}\,d\zeta\right\}. \quad (12)$$

Equation (12) gives a natural decomposition of the field in an axially invariant integrated dielectric waveguide. The residue series of (12) is a sum of surface-wave modes of the guide, complete with excitation amplitudes depending on the incident excitatory field or current. These surface waves satisfy the homogeneous form of the EFIE (10), as we would expect by the conventional definition of surface waves. The branch integral terms in (12) are a continuous superposition of forced radiation field spectral components of the waveguide. They involve spectral excitation amplitudes depending on the incident excitatory field or current and are the subject of a later discussion. Closed-form solutions to the integral equation (10) have been obtained for TE and TM fields supported by the asymmetric slab waveguide [12]; subsequent application of the complex plane analysis described above leads to replication of the surface-wave modes and radiation field, including all excitation amplitudes, as detailed by Marcuse [1].

We now show that the terms in residue series of (12) satisfy the homogeneous form of the transformed EFIE (10). Suppose that the inversion contour of Fig. 3 encloses a simple pole of the transformed field at ζ_p. Near this pole, the transformed field has the form $\vec{e}(\vec{\rho},\zeta) \simeq a_p \vec{e}_p(\vec{\rho})(\zeta - \zeta_p)^{-1}$; substitution into (10) gives

$$a_p(\zeta-\zeta_p)^{-1}\left\{\vec{e}_p(\vec{\rho}) - \int_{CS}\frac{\delta n^2(\vec{\rho}')}{n_c^2}\vec{\vec{g}}_{e\zeta}(\vec{\rho}|\vec{\rho}') \cdot \vec{e}_p(\vec{\rho}')\,dS'\right\} = \vec{e}^{\,i}(\vec{\rho},\zeta). \quad (13)$$

Taking the limit as $\zeta \to \zeta_p$ and noting that $\vec{e}^{\,i}$ is arbitrary, we conclude that $\vec{e}_p$ satisfies

$$\vec{e}_p(\vec{\rho}) - \int_{CS}\frac{\delta n^2(\vec{\rho}')}{n_c^2}\vec{\vec{g}}_{e\zeta_p}(\vec{\rho}|\vec{\rho}')\cdot\vec{e}_p(\vec{\rho}')\,dS' = 0, \qquad \vec{\rho} \in CS \quad (14)$$

so that $\vec{e}_p$ is a surface wave of the waveguide with propagation constant ζ_p. We now show that $\vec{e}$ has the form given above when ζ_p is an eigenvalue of the surface-wave mode EFIE (14); this demonstration allows evaluation of the excitation amplitude coefficient a_p. Operate on (10) with the linear integral operator $\mathscr{L}_p$, defined by

$$\mathscr{L}_p\{\cdot\} = \int_{CS}\frac{\delta n^2(\vec{\rho})}{n_c^2}\vec{e}_p(\vec{\rho})\cdot\{\cdot\}\,dS \quad (15)$$

and use the reciprocal property of the Green's dyad (see [13]) to get

$$\int_{CS}\frac{\delta n^2(\vec{\rho})}{n_c^2}\vec{e}(\vec{\rho})\cdot\vec{e}(\vec{\rho},\zeta)\,dS - \int_{CS}\frac{\delta n^2(\vec{\rho}')}{n_c^2}\vec{e}(\vec{\rho}',\zeta)\cdot\int_{CS}\frac{\delta n^2(\vec{\rho})}{n_c^2} \times \vec{\vec{g}}_{e\zeta}(\vec{\rho}'|\vec{\rho})\cdot\vec{e}_p(\vec{\rho})\,dS\,dS'$$
$$\int_{CS}\frac{\delta n^2(\vec{\rho})}{n_c^2}\vec{e}_p(\vec{\rho})\cdot\vec{e}^{\,i}(\vec{\rho},\zeta)\,dS. \quad (16)$$

For ζ near ζ_p, we can approximate the Green's dyad by the first two terms in its Taylor series expansion about ζ_p. Substitution into (16) and taking the limit $\zeta \to \zeta_p$ gives

$$\lim_{\zeta\to\zeta_p}(\zeta-\zeta_p)\int_{CS}\frac{\delta n^2(\vec{\rho})}{n_c^2}\vec{e}(\vec{\rho},\zeta) \cdot \int_{CS}\frac{\delta n^2(\vec{\rho}')}{n_c^2}\frac{\partial}{\partial\zeta}\vec{\vec{g}}_{e\zeta}(\vec{\rho}|\vec{\rho}')|_{\zeta_p}\cdot\vec{e}_p(\vec{\rho}')\,dS'\,dS = -\int_{CS}\frac{\delta n^2(\vec{\rho})}{n_c^2}\vec{e}_p(\vec{\rho})\cdot\vec{e}^{\,i}(\vec{\rho},\zeta_p)\,dS. \quad (17)$$

Since $\vec{e}^{\,i}$ is arbitrary, we conclude that $\vec{e}(\vec{\rho},\zeta) \simeq a_p\vec{e}_p(\vec{\rho})(\zeta-\zeta_p)^{-1}$ for ζ near ζ_p. This gives

$$a_p = -\frac{1}{c_p}\int_{CS}\frac{\delta n^2(\vec{\rho})}{n_c^2}\vec{e}_p(\vec{\rho})\cdot\vec{e}^{\,i}(\vec{\rho},\zeta_p)\,dS \quad (18)$$

where c_p is a normalization constant. This has the same form as the results of conventional excitation theory [13], [14]. We can derive an alternate form for the excitation amplitude in terms of the impressed current maintaining the excitatory field (see (22))

$$a_p = -\frac{1}{c_p\epsilon_c}\int_{CS}\vec{e}_p(\vec{\rho})\cdot\vec{p}^{\,e}(\vec{\rho},\zeta_p)\,ds. \quad (19)$$

Now $\vec{J}^e = j\omega\vec{P}^e$, and we denote $\vec{e}_p e^{-j\zeta_p z} = \vec{E}_p^+$, so the result can be written

$$a_p = -\frac{1}{j\omega c_p \epsilon_c}\int_{CS} \vec{J}^e(\vec{r})\cdot\vec{E}_p^+(\vec{r})\,dV \tag{20}$$

which is again seen to be in the same form as the result of conventional excitation theory.

We have made the identification of the branch integral in (12) with the radiation field of the waveguide. That is

$$\vec{E}_{\text{RAD}}(\vec{r}) = -\frac{1}{2\pi}\int_{\mathscr{C}_B} \vec{e}(\vec{\rho},\zeta)\,e^{j\zeta z}\,d\zeta \tag{21}$$

where $\vec{e}$ satisfies the forced EFIE (12) for ζ along the branch contour $\mathscr{C}_B$. Spectral components of the radiation field can be decomposed by appropriate decomposition of the impressed field $\vec{e}^i$

$$\vec{e}^i(\vec{\rho},\zeta) = \frac{1}{n_c^2\epsilon_0}\int_{CS} \vec{\vec{g}}_{e\zeta}(\vec{\rho}|\vec{\rho}'')\cdot\vec{p}^e(\vec{\rho}'',\zeta)\,dS''$$

$$= \frac{1}{n_c^2\epsilon_0}\int_{CS} dS'' \int_{-\infty}^{\infty} \vec{\vec{\mathscr{G}}}_g(\vec{\rho}|\vec{\rho}'';\xi,\zeta)\cdot\vec{p}^e(\vec{\rho}'',\zeta)\,d\xi \tag{22}$$

where CS_∞ is the infinite cross section, $|\vec{\rho}| < \infty$, $\vec{p}^e$ is the transform of the impressed polarization, and $\vec{\vec{\mathscr{G}}}_g$ is the integrand in the integral representation of $\vec{\vec{g}}_{e\zeta}$. A unit dyadic polarization point source at location $\vec{\rho}''$ of spatial frequency ξ gives an impressed field $\vec{\vec{\mathscr{G}}}_g/n_c^2\epsilon_0$; this excites a dyadic radiation-field spectral component $\vec{\vec{R}}(\vec{\rho}|\vec{\rho}'';\xi,\zeta)$ which satisfies the following form of the transformed EFIE:

$$\vec{\vec{R}}(\vec{\rho}|\vec{\rho}'';\xi,\zeta) - \int_{CS}\frac{\delta n^2(\vec{\rho}')}{n_c^2}\vec{\vec{g}}_{e\zeta}(\vec{\rho}|\vec{\rho}')\cdot\vec{\vec{R}}(\vec{\rho}'|\vec{\rho}'';\xi,\zeta)\,dS' = \frac{\vec{\vec{\mathscr{G}}}_g(\vec{\rho}|\vec{\rho}'';\xi,\zeta)}{n_c^2\epsilon_0}. \tag{23}$$

Then the total radiation field becomes

$$\vec{E}_{\text{RAD}}(\vec{\rho},z) = -\frac{1}{2\pi}\int_{\mathscr{C}_B} d\zeta\,e^{j\zeta z}\int_{-\infty}^{\infty} d\xi \cdot \int_{CS} \vec{\vec{R}}(\vec{\rho}|\vec{\rho}'';\xi,\zeta)\cdot\vec{p}^e(\vec{\rho}'',\zeta)\,dS''. \tag{24}$$

This result verifies the conjecture [14] that the radiation field of general open boundary waveguide consists of a two-dimensional superposition of spectral components excited by the transformed impressed polarization $\vec{p}^e$.

We now turn to the phenomenon of surface-wave leakage from integrated dielectric waveguides. As noted by Peng and Oliner *et al.* [5], [6], the tri-layered background structure of Fig. 1 is itself a dielectric waveguide. The physical explanation of surface-wave leakage is the coupling of guided modes of the core to guided modes of the asymmetric slab background structure. Under certain conditions, such coupling can occur, resulting in energy transfer (or leakage) from surface waves of the core to surface waves of the background structure; these waves guide energy away from the axis of the waveguide. This phenomenon manifests itself in our mathematical formulation through the presence of simple pole singularities in the reflection and coupling coefficients in the transformed reflected Green's dyad for complex ξ. These singularities occur at those ξ that cause $\lambda = \sqrt{\xi^2+\zeta^2}$ to correspond with an eigenvalue of the TE or TM characteristic equation of the background asymmetric slab guide.

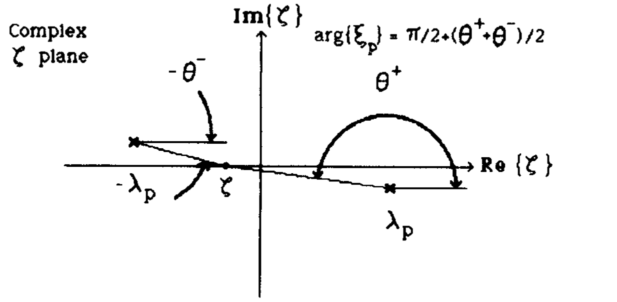

Fig. 4. Complex ζ plane construction defining arguments of the reflected Green's dyad residue series.

It can be shown that the coefficients R_t and C become singular when the parameters p_c, p_s, and p_f satisfy the equation

$$\tanh p_f = \frac{p_f(p_s+p_c)}{p_f^2+p_sp_c} \tag{25}$$

and the coefficients R_n and C become singular when

$$\tanh p_f = \frac{n_f^2p_f(n_c^2p_s+n_s^2p_c)}{n_s^2n_c^2p_f^2+n_f^4p_cp_s} \tag{26}$$

which are the characteristic equations of TE and TM surface waves in the asymmetric slab [1]. Let λ_p denote a surface-wave eigenvalue of the background structure; λ_p must lie in the fourth quadrant of the complex ζ plane so that $\exp(-j\lambda_p r)$ represents a decaying outward-propagating wave. The spatial frequency ξ corresponding to this eigenvalue is $\xi_p^2 = \lambda_p^2 - \zeta^2$. The factor $\exp(j\xi|x-x'|)$ occurring in the residue series contributions to $\vec{\vec{g}}_\zeta^r$ implies $\text{Im}\{\xi_p\} > 0$, we we write $\xi_p = j\sqrt{\zeta-\lambda_p}\times\sqrt{\zeta+\lambda_p}$. From the construction of Fig. 4, we see that in the low-loss limit we have two cases

$$\begin{aligned} \text{Re}\{\zeta\} < \lambda_p \quad & \arg\{\xi_p\} = \pi \\ \lambda_p < \text{Re}\{\zeta\} \quad & \arg\{\xi_p\} = \pi/2. \end{aligned} \tag{27}$$

Then the factor $\exp(j\xi_p|x-x'|)$ in $\vec{\vec{g}}_\zeta^r$ becomes

$$e^{j\xi_p|x-x'|} = \begin{cases} e^{-j|\xi_p||x-x'|} \\ e^{-|\xi_p||x-x'|} \end{cases} \tag{28}$$

for the two cases. This factor represents a wave propagating in the x-direction in the first case, and an exponential decay in the x-direction in the second case. The first case is the regime of leaky modes, in which a surface wave of the core couples into a surface wave of the background structure. The second case is the regime of purely guided modes, where no coupling occurs and the mode is guided

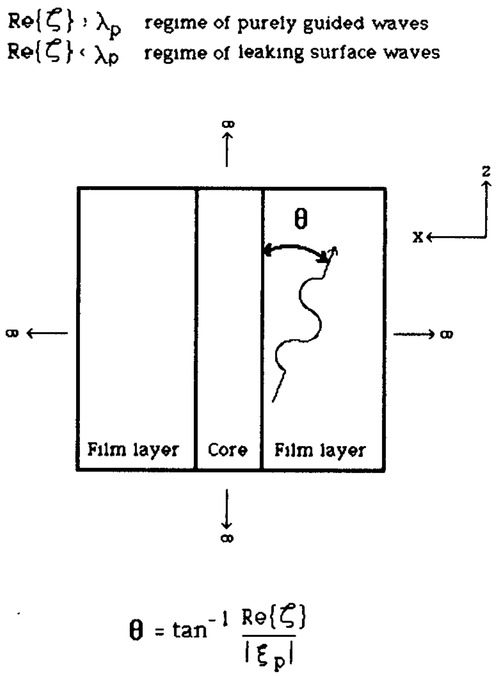

Fig. 5. Surface-wave leakage and leakage angle for integrated dielectric waveguides.

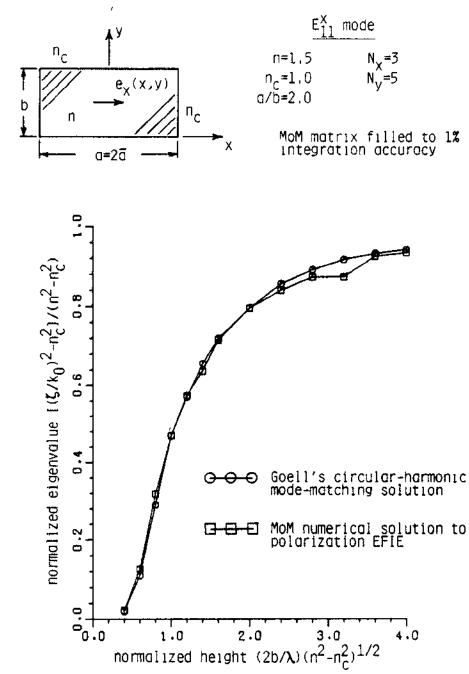

Fig. 6. MoM solution to transformed EFIE for dispersion characteristics of E_{11}^{x} surface-wave mode supported by a step-index dielectric rectangular waveguide.

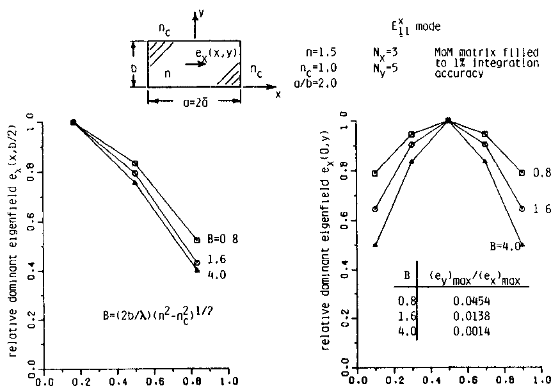

Fig. 7. MoM solution to transformed EFIE for eigenfield distribution of E_{11}^{x} surface-wave mode supported by a step-index dielectric rectangular waveguide.

along the waveguide axis. This situation is illustrated in Fig. 5

IV. Numerical Results

In this section, we present results of the numerical solution of EFIE (14) for the eigenmodes of step-index and graded rectangular strip and rib waveguides. Two techniques are utilized, and the results of each are compared to the results of other formulations of the problem.

If the rectangular components $v = x, y, z$ of the unknown field are expanded in a basis set $\{f_n\}$ and substituted into the surface-wave mode EFIE (14), the spatial integrals can be performed to give

$$\sum_{v} a_{vn}(\zeta)\vec{W}(\vec{\rho},\zeta) = 0, \qquad \vec{\rho} \in CS. \tag{29}$$

Application of a testing operator consisting of dot multiplication by a vector testing function and integration over the guiding region cross section gives the MoM system

$$\sum_{v} \sum_{n=1}^{N} a_{vn}(\zeta) A_{\alpha m}^{vn}(\zeta) = 0,$$

$$\alpha = x, y, z, \qquad m = 1, \cdots, N \tag{30}$$

where the MoM matrix elements are in terms of the spectral integrals which occur in the expressions for the transformed Green's dyad. Solutions $\zeta = \zeta_n$ of (30) are obtained as the roots of $\det[A_{\alpha m}^{vn}(\zeta)] = 0$ for the nth surface-wave eigenmode; expansion coefficients a_{vn} are subsequently determined by deleting one of the dependent equations in system (30), equating the corresponding coefficient to unity, and solving the resulting inhomogeneous system for the remaining coefficients.

The standard MoM solution was implemented by using a pulse function basis and delta functions for testing (point matching). We first present the MoM results for E_{11}^{x} surface waves supported by the isolated rectangular step-index waveguide illustrated in the inset of Fig. 6. The dispersion characteristics displayed in that figure agree well with those of Goell's mode-matching solution [4]. Fig. 7 shows the resultant dominant-field component e_x distribution in the guiding region for several guide dimensions. The next example is that of the E_{11}^{y} surface-wave modes supported by the same waveguide. Once again the dispersion characteristics obtained compare favorably with those of Goell, as illustrated in Fig. 8, and the resultant dominant-field component e_y inside the guiding region is shown in Fig. 9. Our final MoM example is that of E_{11}^{y} surface-wave modes

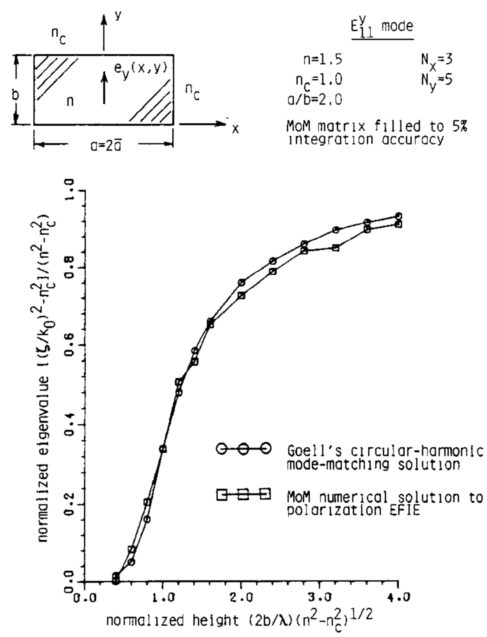

Fig. 8. MoM solution to transformed EFIE for dispersion characteristics of E_{11}^{y} surface-wave mode supported by a step-index dielectric rectangular waveguide.

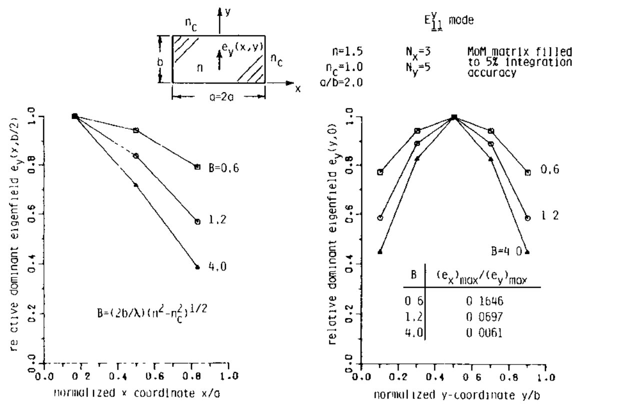

Fig. 9. MoM solution to transformed EFIE for eigenfield distribution of E_{11}^{y} surface-wave mode supported by a step-index dielectric rectangular waveguide.

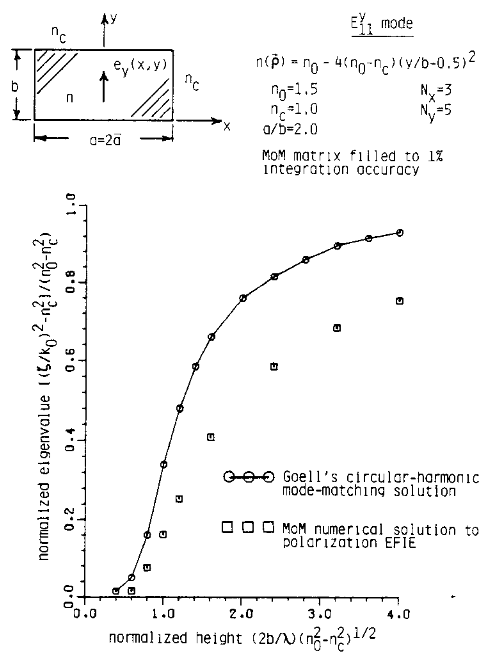

Fig. 10. MoM solution to transformed EFIE for dispersion characteristics of E_{11}^{y} surface-wave mode supported by a graded-index (parabolic along y) dielectric rectangular waveguide.

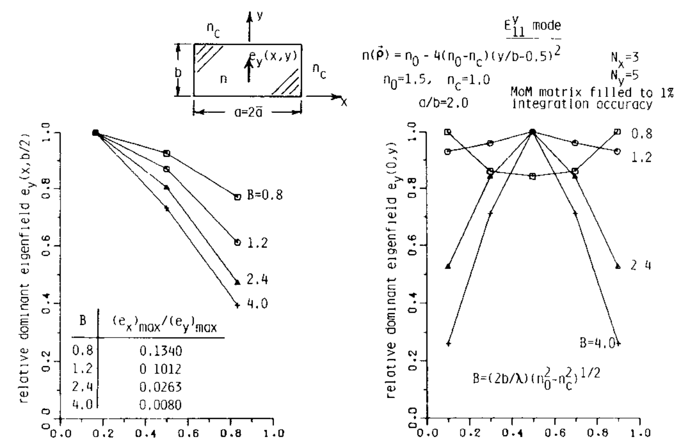

Fig. 11. MoM solution to transformed EFIE for eigenfield distribution of E_{11}^{y} surface-wave mode supported by a graded-index (parabolic along y) dielectric rectangular waveguide.

supported by a graded-index rectangular waveguide in a uniform surround. Here, the refractive index varies in a parabolic fashion along the y-direction as indicated in Fig. 10. The resultant dispersion characteristics are compared to Goell's results for a step-index configuration of a similar contrast. The effect of parabolic core grading on the propagation characteristics of this guide is evident. The dominant-field component distribution in the guide is shown in Fig. 11. Note the anomalous distribution versus y for guides of low contrast. This may indicate an unexplained physical phenomenon, or may be a result of numerical integration inaccuracy (1-percent accuracy was used in all cases).

Quasi-closed-form solutions to the surface-wave mode EFIE (14) can be obtained for the surface waves supported by step-index waveguides with rectilinear boundaries (e.g., the strip and rib configurations). The index contrast is constant within the guiding region and vanishes outside that region. Solutions to Maxwell's equations are constructed in rectangular coordinates by exploiting conventional guided wave theory [13], resulting in the longitudinal TE and TM eigenmodes

$$e_z(x, y) = \begin{Bmatrix} \sin \kappa_x x \\ \cos \kappa_x x \end{Bmatrix} \left[C_1 \cos \kappa_y y + C_2 \sin \kappa_y y \right]$$

$$h_z(x, y) = \begin{Bmatrix} \cos \sigma_x x \\ \sin \sigma_x x \end{Bmatrix} \left[C_3 \cos \sigma_y y + C_4 \sin \sigma_y y \right] \quad (31)$$

in terms of four unknown amplitudes and three unknown eigenvalue parameters (κ_y and σ_y are specified by $\kappa_x^2 + \kappa_y^2 = \sigma_x^2 + \sigma_y^2 = k^2 - \zeta^2$). Transverse-field components are obtained from (31) in the usual manner. Requiring satisfac-

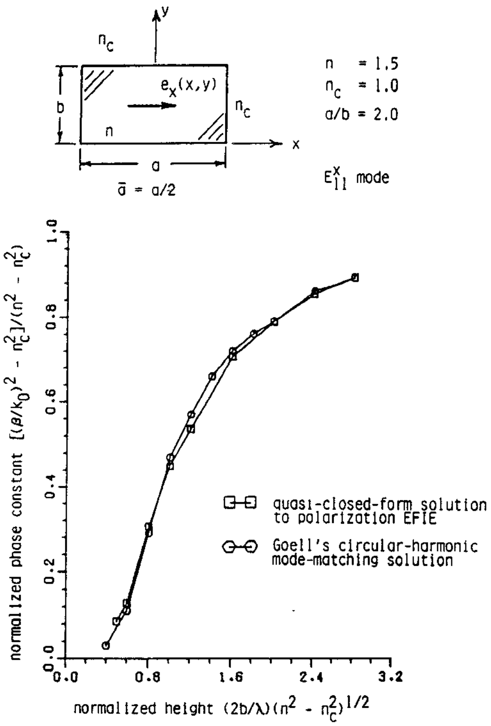

Fig. 12. Dispersion characteristics of E^x_{11} surface-wave mode of a step-index rectangular dielectric waveguide obtained from the transformed EFIE by the quasi-closed-form solution technique.

tion of EFIE, (14) leads to

$$\sum_{n=1}^{4} C_n W_n^{(\alpha)}(\kappa_x, \sigma_x, \zeta, x, y) = 0 \quad \text{for} \quad \alpha = x, y, z, \quad \vec{r} \in CS. \tag{32}$$

The W_n are given by Sommerfeld integrals following closed-form integration on the primed spatial variables. Since this formulation is based on a potentially exact solution to Maxwell's equations, the component equations (32) can be matched at four points within the waveguide, leading to a system of three homogeneous matrix equations. These equations can be solved simultaneously (e.g., by the three-dimensional Newton's method) to yield the eigenvalue parameters κ_x, σ_x, and ζ of the surface-wave eigenmode. We can solve at this point for the amplitude constants of (31) to completely specify the eigenfields.

This technique has been implemented for the E^x_{11} surface-wave modes of the uniform rectangular dielectric waveguide with uniform surround illustrated in the inset of Fig. 12. The resultant dispersion characteristics are compared with the results obtained by Goell [4], and excellent agreement is observed, even in the near cutoff regime where the approximate solutions obtained by Marcatili's method [3] and the EDC method [5] fail. The associated eigenfield distributions are illustrated in Fig. 13, where the expected confinement increase with guide dimensions is evident. This technique was also implemented for the rib waveguide shown in the inset of Fig. 14. Eigenvalues obtained are compared with the results of the EDC method for various film thicknesses; these compare favorably for the principle E^x_{11} mode. In this case, the reflected Green's dyad was approximated by its residue series at the

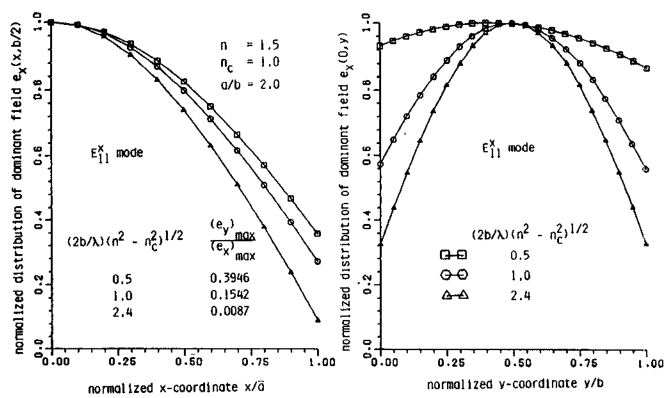

Fig. 13. Distribution of the dominant-field component $e_x(x, y)$ for the E^x_{11} surface-wave mode of a step-index rectangular dielectric waveguide obtained from the transformed EFIE by the quasi-closed-form solution technique.

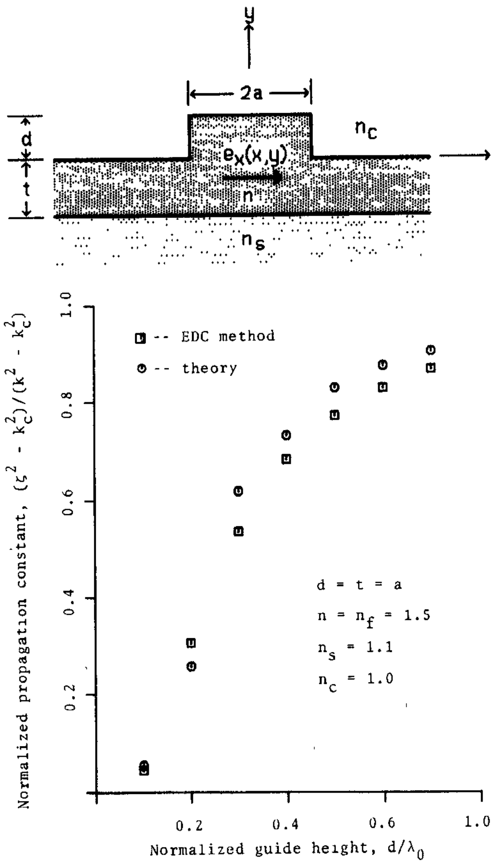

Fig. 14. Dispersion characteristics of E^x_{11} surface-wave mode of a step-index rectangular rib dielectric waveguide obtained from the transformed EFIE by the quasi-closed-form solution technique.

poles of the integrand, and the branch integral contribution was neglected (see Section II). The adequacy of this approximation is justified by the results presented; since the residues yield a closed-form contribution, this approximation is potentially of great usefulness elsewhere.

V. Conclusions

We have presented an integral formulation for use in the analysis of a broad class of integrated dielectric waveguiding systems. In the case of axially uniform waveguides, the

EFIE can be reduced in dimension by Fourier transforming on the axial variable. Analysis of the transformed EFIE in the complex transform variable plane leads to identification of two components making up the total core field: the surface-wave modes and the radiation field. The resultant expression for the waveguide core field yields surface-wave model excitation amplitudes in agreement with the results of conventional excitation theory, as well as a new formulation of the radiation field of the waveguide. We are also able to formulate a new criterion for prediction of the excitation of Oliner's leakage waves in the layered background environment of the integrated waveguide.

The transformed EFIE has been used as a basis for numerical solution for the surface waves supported by rectangular strip and rib waveguides. Standard MoM solutions for rectangular guides in a uniform surround yielded good agreement with Goell's results in the case of step-index guides, and yielded new results for parabolically graded guides. A quasi-closed-form solution technique was also applied to the EFIE, and numerical results obtained compare favorably for the case of isolated step-index rectangular guides and step-index rib guides.

Further numerical results are anticipated using variational techniques, as well as the Neumann series method. Numerical and analytical results on the radiation field of integrated waveguides are being pursued, and the application of the three-dimensional EFIE to the interesting problem of truncated guides is also being explored.

Appendix
Green's Dyad Reflection and Coupling Coefficients

The reflection and coupling coefficients appearing in the Green's dyad component integrals are detailed below. In the following, we define

$$N_{fc} = N_{cf}^{-1} = \frac{n_f}{n_c} \quad N_{sf} = N_{fs}^{-1} = \frac{n_s}{n_f}.$$

Coefficients in Green's Dyad

$$R_t(\lambda) = R^t_{fc} + \frac{T^t_{cf} R^t_{sf} T^t_{fc} e^{-2p_f t}}{1 - R^t_{cf} R^t_{sf} e^{-2p_f t}}$$

$$R_n(\lambda) = R^n_{fc} + \frac{T^n_{cf} R^n_{sf} T^n_{fc} e^{-2p_f t}}{1 + R^n_{fc} R^n_{sf} e^{-2p_f t}}$$

$$C(\lambda) = C_1 + \frac{T^n_{fc}\left(R^n_{sf} N^2_{cf} C_1 + C_2\right) e^{-2p_f t}}{1 + R^n_{fc} R^n_{sf} e^{-2p_f t}}$$

$$C_1(\lambda) = \frac{N^2_{fc}\left(N^2_{fc} - 1\right) T^t_{cf}}{N^2_{fc} p_c + p_f} \, \frac{1 + R^t_{sf} e^{-2p_f t}}{1 - R^t_{cf} R^t_{sf} e^{-2p_f t}}.$$

Factors Associated with the Cover/Film Interface

$$R^t_{fc}(\lambda) = -R^t_{cf}(\lambda) = \frac{p_c - p_f}{p_c + p_f} \quad R^n_{fc}(\lambda) = \frac{N^2_{sf} p_f - p_s}{N^2_{sf} p_f + p_s}$$

$$R^t_{fc}(\lambda) = \frac{2N^2_{fc} p_f}{p_c + p_f} \qquad T^t_{cf}(\lambda) = \frac{2N^2_{cf} p_c}{p_c + p_f}$$

$$T^n_{fc}(\lambda) = \frac{2p_f}{N^2_{cf} p_f + p_c} \qquad T^n_{cf}(\lambda) = \frac{2p_c}{N^2_{fc} p_c + p_f}.$$

Factors Associated with the Film/Substrate Interface

$$R^t_{sf}(\lambda) = \frac{p_f - p_s}{p_f + p_s} \qquad T^t_{fs}(\lambda) = \frac{2N^2_{fs} p_f}{p_f + p_s}$$

$$R^n_{sf}(\lambda) = \frac{N^2_{sf} p_f - p_s}{N^2_{sf} p_f + p_s} \qquad T^n_{fs}(\lambda) = \frac{2p_f}{N^2_{sf} p_f + p_s}.$$

References

[1] D. Marcuse, *Theory of Dielectric Optical Waveguides.* New York: Academic Press, 1974, ch. 1.

[2] R. C. Pate and E. F. Keuster, "Fundamental propagation modes on a dielectric waveguide of arbitrary cross section," Sci. Rep. no. 45, U.S. Army Research Office, Contract no. DAA 29-78-C-1073, Electromagnetics Laboratory, Univ. of Colorado, Boulder, CO, Feb. 1979.

[3] E. A. J. Marcatili, "Dielectric rectangular waveguide and directional coupler for integrated optics," *Bell Syst. Tech. J.*, vol. 48, no. 9, pp. 2071–2102, Sept. 1969.

[4] J. E. Goell, "A circular-harmonic computer analysis of rectangular dielectric waveguides," *Bell Syst. Tech. J.*, vol. 48, no. 9, pp. 2133–2160, Sept. 1969.

[5] S-T. Peng and A. A. Oliner, "Guidance and leakage properties of a class of open dielectric waveguides: Part I—Mathematical formulations," *IEEE Trans. Microwave Theory Tech.*, vol. MTT-29, pp. 843–855, Sept. 1981.

[6] A. A. Oliner, S-T. Peng, T-I. Hsu, and A. Sanchez "Guidance and leakage properties of a class of open dielectric waveguides: Part II—New physical effects," *IEEE Trans. Microwave Theory Tech.*, vol. MTT-29, pp. 855–869, Sept. 1981.

[7] B. Z. Katsenelenbaum, "On the propagation of electromagnetic waves along an infinite dielectric cylinder at low frequencies," *Dokl. Akad. Nauk. SSSR*, vol. 58, no. 7, 1947.

[8] D. E. Livesay and K-M. Chen, "Electromagnetic fields induced inside arbitrarily shaped biological bodies," *IEEE Trans. Microwave Theory Tech.*, vol. MTT-22, pp. 1273–1280, Dec. 1974.

[9] D. R. Johnson and D. P. Nyquist, "Integral-operator analysis for dielectric optical waveguides—Theory and application," in *Digest of National Radio Science (URSI) Meet.* (Univ. of Colorado, Boulder, CO), Nov. 1978, p. 104.

[10] A. Sommerfeld, *Partial Differential Equations in Physics.* New York: Academic Press, 1964, pp. 236–265.

[11] A. D. Yaghjian, "Electric dyadic Green's functions in the source region," *Proc.. IEEE*, vol. 68, pp. 284–263, Feb. 1980.

[12] J. S. Bagby, "Integral equation analysis of integrated dielectric waveguides," Ph.D. dissertation, Michigan State Univ., 1984.

[13] R. E. Collin, *Field Theory of Guided Waves.* New York: McGraw-Hill, 1960, p. 492.

[14] D. P. Nyquist, D. R. Johnson, and S-V Hsu, "Orthogonality and amplitude spectrum of radiation modes along boundary waveguides," *J. Opt. Soc. Am.*, vol. 71, pp. 49–54, Jan. 1981.

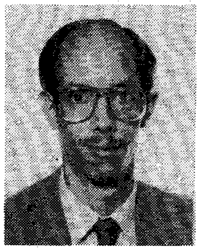

Jonathan S. Bagby (S'78–M'84) received the B. S. Degree with high honors in electrical engineering from Michigan State University as a Ford Fellow in 1980. He received the M.S. degree in electrical engineering from Ohio State University in 1981, where he was a University Fellow. He received the Ph.D. degree in 1984 as Dean's Distinguished Fellow in electrical engineering at Michigan State University.

In 1981, he was a Research Assistant at the ElectroScience Laboratory in Columbus, OH, where his thesis dealt with radar target identification using natural resonances. From 1982 to 1984, he was a Research Assistant at Michigan State University, where his dissertation involved guided waves in open boundary structures. In 1984, the joined the faculty at the University of Texas at Arlington, where he is an Assistant Professor. His current interests include open boundary waveguides, microstrip devices, and numerical methods in electromagnetics.

Dr. Bagby is a member of Sigma Xi, Phi Kappa Phi, Tau Beta Pi, and Eta Kappa Nu. He was the first recipient in 1984 of the Union of Radio Scientists Graduate Travel Award, and received the Excellence in Teaching Citation from Michigan State University in 1982.

Dennis P. Nyquist (S'63–M'67) was born in Detroit, MI, on August 18, 1939. He received the B.S.E.E. and M.S.E.E. degrees in 1961 and 1964, respectively, and the Ph.D. degree in electrical engineering from Michigan State University, East Lansing, in 1966.

Prior to obtaining the Ph.D. degree, he was a Research Engineer at the Ford Research Laboratories. He held an Engineering College Predoctoral Fellowship during his doctoral program at Michigan State University, East Lansing. He joined the Electrical Engineering Faculty at Michigan State University as an Instructor in 1966, became Assistant Professor in 1967, Associate Professor in 1970, and Professor in 1979. He has published a number of papers on electromagnetic radiation, antennas, and scattering. His current research interests include target discrimination with transient waveforms and guided-wave optics.

Dr. Nyquist is a member of Commission B of the International Scientific Radio Union, the American Association for the Advancement of Science, Sigma Xi, and Phi Kappa Phi. He was the recipient of the Michigan State University Teacher–Scholar Award in 1969.

Byron C. Drachman received the B.S. degree in electrical engineering from the University of Illinois, the M.S. degree in applied mathematics from the University of Arizona, and the Ph.D. degree in pure mathematics (algebraic topology) from Brown University, in 1960, 1962, and 1966 respectively.

He was at the Centro de Investigacion del IPN, Mexico City, from 1966 to 1970. He has been at Michigan State University since 1971, where he is a Professor of mathematics.